

Automatic determination of the planetary boundary layer height using lidar: One-year analysis over southeastern Spain

M. J. Granados-Muñoz,^{1,2} F. Navas-Guzmán,^{1,2} J. A. Bravo-Aranda,^{1,2}
 J. L. Guerrero-Rascado,^{1,2,3} H. Lyamani,^{1,2} J. Fernández-Gálvez,^{1,2}
 and L. Alados-Arboledas^{1,2}

Received 25 January 2012; revised 11 August 2012; accepted 14 August 2012; published 22 September 2012.

[1] The planetary boundary layer (PBL) height is a key variable in climate modeling and has an enormous influence on air pollution. A method based on the wavelet covariance transform (WCT) applied to lidar data is tested in this paper as an automated and non-supervised method to obtain the PBL height. The parcel and the Richardson number methods applied to radiosounding data and the parcel method applied to microwave radiometer temperature profiles are used as independent measurements of the PBL height in order to optimize the parameters required for its detection using the WCT method under different atmospheric conditions. This optimization allows for a one-year statistical analysis of the PBL height at midday over Granada (southeastern Spain) from lidar data. The PBL height showed a seasonal cycle, with higher values in summer and spring while lower values were found in winter and autumn. The annual mean was 1.7 ± 0.5 km a.s.l. during the study period. The relationship of the PBL height with aerosol properties is also analyzed for the one-year period.

Citation: Granados-Muñoz, M. J., F. Navas-Guzmán, J. A. Bravo-Aranda, J. L. Guerrero-Rascado, H. Lyamani, J. Fernández-Gálvez, and L. Alados-Arboledas (2012), Automatic determination of the planetary boundary layer height using lidar: One-year analysis over southeastern Spain, *J. Geophys. Res.*, 117, D18208, doi:10.1029/2012JD017524.

1. Introduction

[2] The planetary boundary layer (PBL) is the part of the troposphere directly influenced by the Earth's surface and it responds to surface forcings with a time scale of about an hour or less [Stull, 1988]. The height of this layer is a fundamental quantity for the description of vertical mixing processes in the lower part of the troposphere and it exerts a strong influence in the environmental state at the surface. The PBL height is highly variable in time and space, ranging from a few hundred meters to several kilometers with diurnal and seasonal cycles. The PBL height and its cycles are key parameters controlling air pollution because they determine the available volume for pollutants dispersion [Seibert *et al.*, 2000] and are crucial for air quality studies. Accurate estimates of the PBL height are also important in climate modeling, as the PBL properties and processes influence the

information provided by the regional and global climate models [Holtslag, 2006]. Also, a correct modeling of the PBL height in climate models is fundamental since pollutants present different behavior in the different atmospheric layers, with longer life time and transport range in the free troposphere.

[3] Because of its importance in weather forecasting, environmental monitoring and climate modeling, statistical studies of the PBL height provide valuable information. However, most studies have usually focused on local scale and/or short-term [Sicard *et al.*, 2006; Pal *et al.*, 2010] primarily due to the complexity of the methodology involved to determine the PBL height. Different methodologies allow estimates of the PBL height depending on the instrumentation and the tracers used. Commonly used methods include the Richardson number method [Vogelezang and Holtslag, 1996; Menut *et al.*, 1999] based on radiosounding wind and temperature profile data, the parcel method [Holzworth, 1964] using radiosounding temperature profile data, and the derivative and non-derivative methods used for lidar with atmospheric aerosol as a tracer [Baars *et al.*, 2008].

[4] Improvements in PBL height determinations include the use of automatic algorithms. The wavelet covariance transform (WCT) method applied to lidar observations using atmospheric aerosol as a tracer represents a promising tool for automatic PBL height detection [Morille *et al.*, 2007; Baars *et al.*, 2008; Pal *et al.*, 2010]. In fact, this methodology has already been successfully implemented for ceilometers

¹Centro Andaluz de Medio Ambiente, Universidad de Granada, Junta de Andalucía, Granada, Spain.

²Departamento de Física Aplicada, Universidad de Granada, Granada, Spain.

³Évora Geophysics Centre, University of Évora, Évora, Portugal.

Corresponding author: M. J. Granados-Muñoz, Departamento de Física Aplicada, Universidad de Granada, Av. Fuentenuueva s/n, ES-18071 Granada, Spain. (mjgranados@ugr.es)

[Haefelin *et al.*, 2012]. Moreover, automatic PBL height determinations with the WCT method will allow for global-scale monitoring of the PBL height from lidar networks such as EARLINET (European Aerosol Research Lidar Network) [Bösenberg *et al.*, 2001], MPLNET (Micro-Pulsed Lidar Network) [Welton *et al.*, 2001] and ADNET (Asian Dust Network) [Murayama *et al.*, 2001].

[5] The aim of this work is to step forward on an automatic algorithm for determining the PBL height from lidar measurements with a method based on the WCT. Parameters used in the WCT method are optimized using independent PBL height estimates from the parcel and the Richardson number method with radiosounding data as well as the parcel method with atmospheric temperature profiles measured by a co-located passive microwave radiometer. The optimized WCT-based method is used to compute the PBL height from lidar data at midday over the city of Granada (southeastern Spain) during an entire year and the relationship of this height with the aerosol optical depth and surface extinction coefficient is also analyzed.

[6] This paper is organized as follows: Section 2 briefly describes the experimental site and instruments; Section 3 describes methodologies used for PBL height detection; the optimization of the WCT method from independent measurements of the PBL height is discussed in Section 4; Section 5 focuses on the one-year analysis of the PBL height at midday over Granada and its relationship with aerosol properties; and conclusions are drawn in Section 6.

2. Experimental Site and Instruments

[7] Data used in this work were collected at the atmospheric experimental station of the University of Granada, located on the Andalusian Centre for Environmental Research (37.16°N, 3.60°W, 680 m a.s.l.). Granada is a medium-size and a non-industrialized city of around 250000 inhabitants (twice including its metropolitan area). The city is located in a natural basin surrounded by mountains, with the highest ones located at the southeast of the basin (over 3000 m a.s.l.). Moreover, it is 200 km away from the African continent and approximately 50 km away from the western Mediterranean basin. Due to its location within the Iberian Peninsula, the study area is affected by air masses coming from the Atlantic Ocean, the European and African continents and less frequently from the Mediterranean Sea [Alados-Arboledas *et al.*, 2003; Lyamani *et al.*, 2010]. Differences in temperature and relative humidity among these air masses induce remarkable changes in surface variables throughout the year. The area presents a Mediterranean-continental climate, with cool winters and hot summers. Average annual rainfall is 361 mm, falling mainly during spring and winter. The diurnal thermal oscillation is quite high through the year, often reaching up to 20 K and producing strong variations in relative humidity during the day, with minimum values at noon and maximum at sunrise. Seasonal changes of relative humidity are also high with mean values varying from 45% in summer to 75% in winter. The bowl-like topography of the Granada basin and its climate favors winter-time thermal inversions and the predominance of very low wind speeds. The local aerosol sources are mainly traffic (particularly diesel vehicles) together with re-suspended material from the ground mostly during the dry season, while

domestic heating (based on fuel oil combustion) represents an additional source of anthropogenic aerosols in winter.

[8] A Raman-lidar (LR331D400, Raymetrics S.A.), operating at the station since 2005, was used for profiling the atmospheric aerosol. It is configured in a monostatic biaxial alignment pointing vertically to the zenith. The transmission system consists of a pulsed Nd:YAG with fundamental emission at 1064 nm. Additional emissions at 532 and 355 nm are obtained from second and third harmonic generators. The backscattered signal is collected by a 40 cm-diameter Cassegrainian telescope and split into seven spectral channels using dichroic mirrors, interference filters and a polarizing beamsplitter cube. The detection and spectral selection is performed at four channels corresponding to elastic wavelengths at 1064, 532 (parallel-polarized and perpendicular-polarized) and 355 nm, and three additional channels for the Raman signals at 607 nm (N₂ Raman-shifted signal from 532 nm), 408 nm (water vapor Raman-shifted signal from 355 nm) and 387 nm (N₂ Raman-shifted signal from 355 nm). The instrument is operating with a spatial vertical resolution of 7.5 m. Due to the instrument setup, the incomplete overlap limits the lowest possible detection height at 500 m above the system for the 532 nm wavelength used in this study [Navas-Guzmán *et al.*, 2011]. The Raman lidar was incorporated to EARLINET (European Aerosol Research Lidar Network) [Bösenberg *et al.*, 2001] in April 2005. It has taken part of the EARLINET-ASOS (European Aerosol Research Lidar Network - Advanced Sustainable Observation System) project and currently is involved in the ACTRIS (Aerosols, Clouds, and Trace gases Research Infrastructure Network) European project. Further details in relation to this instrument can be found in Guerrero-Rascado *et al.* [2008, 2009].

[9] Tropospheric temperature and humidity profiles were measured by a ground-based multifrequency passive microwave radiometer (RPG-HATPRO, Radiometer Physics GmbH). This instrument performs measurements of the sky brightness temperature in a continuous and automated way with a radiometric resolution between 0.3 and 0.4 K root mean square error at 1.0 s integration time. The radiometer uses direct detection receivers within two bands: 22–31 and 51–58 GHz. The first band contains channels providing information about the humidity profile of the troposphere, while the second band contains information about the temperature profile. The retrieval of both temperature and humidity profiles from brightness temperature are done by inversion algorithms [Rose *et al.*, 2005]. Temperature data are provided with 0.1 K precision and the accuracy of the temperature retrievals has a mean value of up to 0.8 K within the boundary layer. Tropospheric profiles are obtained from the surface up to 10 km using 39 heights with vertical resolution ranging from 10 m near the surface to 1000 m for altitudes higher than 7 km. For heights below 3 km a.s.l., where the PBL is usually located over Granada, data at 25 points with resolution between 10 and 200 m are provided.

[10] During summer and autumn 2011, radiosounding data were also available at the site. A total of eight radiosoundings at midday were launched with simultaneous measurements of the lidar system and the microwave radiometer. Radiosounding data were obtained with lightweight weather radiosondes (DFM-06, GRAW Radiosondes) that provide temperature (resolution 0.01°C, accuracy 0.2°C),

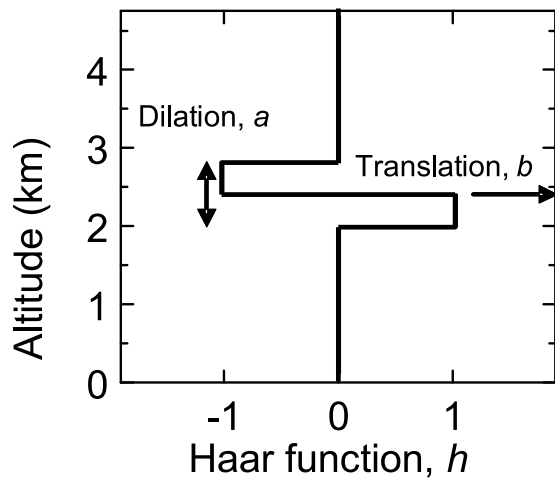


Figure 1. Haar function.

pressure (resolution 0.1 hPa, accuracy 0.5 hPa), humidity (resolution 1%, accuracy 2%) and wind speed (resolution 0.1 m/s, accuracy 0.2 m/s). Data acquisition and processing were performed by Grawmet5 software and a GS-E ground station from the same manufacturer.

[11] The site is also equipped with a meteorological station and surface data are used as the reference for additional instruments. Temperature at ground level is monitored at one-min time resolution with an accuracy of 0.6°C and 0.01°C precision (HMP60, Vaisala).

[12] Atmospheric extinction coefficient at 637 nm during the monitoring period was computed from data provided by a MultiAngle Absorption Photometer (MAAP-5012, Thermo ESM Andersen Instruments) and an integrating nephelometer (model 3563, TSI Inc.) as described in *Lyamani et al.* [2008, 2010]. The uncertainty of the extinction coefficient is lower than 20%. Moreover, aerosol optical depth at 675 nm using AERONET (Aerosol Robotic Network) level 2 data was obtained from Sun photometer (CE-318-4, Cimel Electronique) measurements [*Holben et al.*, 1998]. The uncertainty in the retrieval of aerosol optical depth under cloud free conditions is ± 0.01 for wavelengths larger than 440 nm and ± 0.02 for shorter wavelengths [*Eck et al.*, 1999].

3. Methodology

3.1. Detection of the PBL Height Based on the Wavelet Covariance Transform (WCT)

[13] There are several methods to determine the PBL height using a lidar system, which are based on the assumption that aerosol is much more abundant within the PBL than in the free troposphere. Therefore it is necessary to find the height where aerosol concentration abruptly decreases. For lidar systems, typically the detected backscattered light is much higher within the PBL than in the free troposphere due to the higher abundance of particles. A parameter commonly used with lidar systems is the range-corrected signal (RCS), defined as:

$$RCS(z) = [P(z) - P_{BG}] \cdot z^2 \quad (1)$$

where the lidar signal $P(z)$ is expressed as follows:

$$P(z) = O(z) \frac{C}{z^2} [\beta^a(z) + \beta^m(z)] \cdot T^2(z) + P_{BG} \quad (2)$$

being $O(z)$ the overlap function, C a function related to the system, z the distance, β the backscatter coefficient (for aerosol and molecular components indicated by superscripts “a” and “m” respectively), T the atmospheric transmittance and P_{BG} the background signal.

[14] There are mainly two methodologies to identify the transition zone where the aerosol concentration abruptly decreases, which are known as derivative and non-derivative methods. The variance method [*Hooper and Eloranta*, 1986] is an example of a non-derivative method. On the other hand, derivative methods are widely extended and accepted [*Vaughan et al.*, 2005; *Sicard et al.*, 2006]; some examples are the gradient method and the inflexion point method [*Hayden et al.*, 1997; *Flamant et al.*, 1997; *Menut et al.*, 1999], the fitting method [*Steyn et al.*, 1999] and the WCT method [*Cohn and Angevine*, 2000; *Brooks*, 2003; *Morille et al.*, 2007; *Baars et al.*, 2008]. The WCT method is suitable under many meteorological situations and valid for all seasons. Moreover it has the advantage of being less affected by noise than any other method [*Baars et al.*, 2008]. Additionally, it can be easily automated for continuous PBL height detection from lidar data.

[15] The WCT, $W_f(a, b)$, is defined as:

$$W_f(a, b) = \frac{1}{a} \int_{z_b}^{z_t} RCS(z) h\left(\frac{z-b}{a}\right) dz \quad (3)$$

where z_b and z_t are the lower and upper limits of the back-scattered signal and h is the Haar function (Figure 1),

$$h\left(\frac{z-b}{a}\right) = \begin{cases} +1, & b - \frac{a}{2} \leq z \leq b \\ -1, & b \leq z \leq b + \frac{a}{2} \\ 0, & \text{elsewhere} \end{cases} \quad (4)$$

a is a parameter called dilation related to the extent of the step function and b is the translation, which indicates the location of the step. Due to the overlap of the lidar system, z_b is limited. For the 532 nm wavelength used in this study, the complete overlap height is several hundred meters over the station, but at 500 m the information is reliable for detecting structures since the relative deviation from the complete overlap is below 40% for the system [*Navas-Guzmán et al.*, 2011]. Therefore, the obtained PBL heights from lidar data are only reliable above this altitude. Finally, for computing $W_f(a, b)$, the RCS is normalized by the maximum value below 1000 m a.g.l., usually its maximum value within the PBL [*Baars et al.*, 2008].

[16] The WCT measures the similarity between the normalized RCS and h , presenting maxima when b coincides with the height at which an abrupt change in RCS occurs. Therefore, this methodology allows for the detection of aerosol layers in the atmosphere. To identify the layer corresponding to the PBL height, several criteria are proposed in the literature. In some cases, the PBL height is estimated by the value of b corresponding to the largest maximum of the W_f vertical profile [*Brooks*, 2003; *Morille et al.*, 2007]. In some other

cases, it is determined by the value of b corresponding to the first maximum of the W_f vertical profile above the surface [Baars *et al.*, 2008]. The uncertainty in the PBL height by the WCT method was half of the dilation according to the sensitivity analysis performed in this work using different dilation values with a synthetic RCS profile.

3.2. Richardson Number Method

[17] The most extended method to determine the PBL height from radiosounding data is based on the Richardson number, but it can only be used under convective conditions. The Richardson number, R_{ib} , is defined as [Stull, 1988]:

$$R_{ib}(z) = \frac{g(z - z_0)[\theta(z) - \theta(z_0)]}{\theta(z)[u(z)^2 + v(z)^2]} \quad (5)$$

being g the gravity acceleration, z_0 the altitude of measurement location above sea level, θ the potential temperature and $u(z)$ and $v(z)$ the wind zonal and meridional components. The PBL height is obtained as the height where the Richardson number equals the critical Richardson number, 0.21 [Vogelezang and Holtslag, 1996; Menuet *et al.*, 1999]. At heights where R_{ib} is higher than the critical value, the atmosphere is considered to be free of turbulences (free troposphere).

3.3. Parcel or Holzworth Method

[18] The parcel or Holzworth method [Holzworth, 1964] is also widely used for PBL height detection using radiosounding data, with the advantage of no need for wind profile. The PBL height is determined from the intersection between the dry adiabatic starting at the surface temperature and the temperature profile [Holzworth, 1964; Seibert *et al.*, 2000]. This height represents the equilibrium level of a hypothetical rising parcel of air representing a thermal. This method strongly depends on the surface temperature and a high uncertainty in the estimated height may result in situations without a pronounced inversion at the convective PBL top. Using the microwave radiometer, the mixing height is determined at the intersection between the dry adiabatic starting at the surface temperature and the interpolated temperature profile provided by the microwave radiometer. As for radiosoundings, the surface temperature is measured from a collocated meteorological station.

4. Optimization of the WCT Method for PBL Height Detection

[19] Lidar system characteristics together with atmospheric conditions may limit the PBL height detection from lidar measurements. Therefore it is important to identify when the detection is possible and then optimize the methodology. For the WCT method, selecting an appropriate dilation parameter, a , is critical; small values result in a noisy WCT profile while large values may overlook some structures. The optimum value would be equal to the depth of the transition zone between the PBL and the free troposphere but this is usually unknown [Brooks, 2003]. To distinguish the PBL top among the different layers detected by the WCT method, the criteria proposed by Baars *et al.* [2008] using the first maximum in the W_f vertical profile

from the surface was used. To distinguish among strong and weak gradients a threshold value for the WCT profile is introduced. Then the PBL height is determined from the lowest height above ground with a local maximum on the WCT profile exceeding this threshold [Baars *et al.*, 2008]. Dilation values between 200 and 450 m provide good results depending on the lidar vertical resolution [Baars *et al.*, 2008; Pal *et al.*, 2010]. The threshold value for the WCT profile varies with dilation but values between 0.04 and 0.08 are usually satisfactory [Baars *et al.*, 2008]. Different combinations of dilation and threshold value, based on these range of values, were used to compute PBL height from lidar data and compared to independent PBL heights from the parcel and the Richardson number methods with radiosounding data in order to establish an optimum pair of values of a and the threshold value for the automatic detection of the PBL. This comparison revealed that the detection of the PBL height gets particularly complex in the presence of stratification within the PBL or lofted aerosol layers coupled with the PBL. Under these circumstances the selection of dilation and the threshold value becomes critical and not always satisfactory for PBL height detection.

[20] A couple of examples are shown in Figures 2 and 4. Time series of the RCS as well as the normalized RCS (arbitrary units) at 532 nm profiles for 25 July 2011 from 11:00 to 11:30 UTC are shown in Figure 2a, including the WCT profile for $a = 300$ m. As it can be observed, several maxima appear in the WCT profile due to stratification within the PBL and a decoupled aerosol layer at 4 km a.s.l., making difficult to identify the one corresponding to the PBL height. Independent measurements using radiosounding data with the parcel and the Richardson number methods set the PBL height at 3.1 and 3.2 km a.s.l. respectively. Also lidar additional information, such as the evolution of the RCS along the morning (Figure 2b) indicates that the PBL height is over 3 km a.s.l.

[21] The appropriate combination of dilation and threshold value can provide the PBL height with differences below 100 m compared to values from radiosounding (Figure 3). Several combinations provided satisfactory results. Nevertheless lower dilations are recommended to improve vertical resolution. Particularly on this date, $a = 225$ m with a 0.04 threshold and $a = 300$ m and 0.05 threshold were the lower dilations that fulfilled the criteria establishing the PBL height at 3.1 km a.s.l.

[22] On the other hand, an example of those cases when it is not possible to obtain satisfactory PBL heights is shown in Figure 4. It corresponds to 25 November 2011 from 12:10 to 12:40 UTC. The PBL height using lidar data is set at 1.2 km a.s.l. for every combination of a and threshold value; while 1.6 km a.s.l. is obtained using the parcel and the Richardson number method with radiosounding data. Therefore, additional information is needed in this case.

[23] The complete comparison was performed with data from eight radiosondes launched at midday over Granada during spring and autumn 2011 in coincidence with the lidar measurements. From this comparison $a = 300$ m and 0.05 threshold value were selected as optimum values for PBL height detection. The agreement between the parcel and the Richardson method from radiosounding profiles were within 300 m. The comparison of PBL heights using the optimized

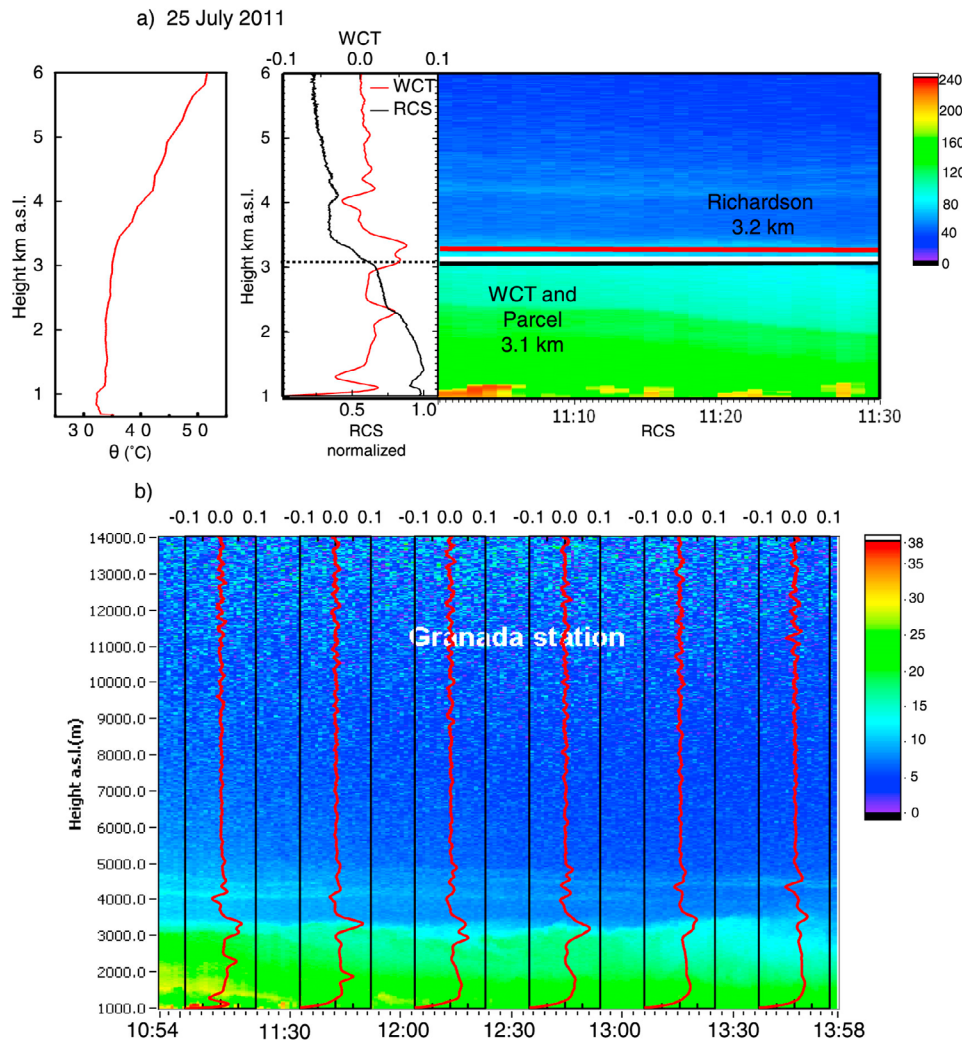


Figure 2. (a) From left to right, potential temperature (θ) profile from radiosounding; WCT for $a = 300$ m and normalized RCS at 532 nm vertical profiles; and time series of the RCS (arbitrary units) for 25 July 2011 between 11:00 and 11:30 UTC. The dotted line indicates the maximum of the WCT corresponding to the PBL height. Lines represent the PBL height obtained by the parcel, the Richardson number and the WCT method in black, red and white, respectively. (b) Time series of the RCS for 25 July 2012 between 10:54 and 13:58. The red lines represent the WCT profile each half an hour.

WCT method and the Richardson method is shown in Figure 5.

[24] The comparison analysis with the eight radiosoundings was also performed with the criteria proposed by Brooks, [2003] and Morille *et al.*, [2007] using a range of dilations from small to large values and no threshold to identify the most significant gradients. Results for the eight cases were completely equivalent to those obtained with the criteria proposed by Baars *et al.* [2008]. Therefore this latter criterion was applied because the implementation of the method is more straightforward.

[25] A comparison between PBL height retrieval from microwave radiometer data and radiosounding data with the parcel method has been also performed. When comparing PBL heights derived from radiosounding and microwave radiometer data differences varies from less than 0.1 up to 0.4 km. The mean value obtained for the eight radiosoundings

compared to simultaneous microwave radiometer temperature profiles was 0.2 ± 0.2 km.

[26] To extend the optimization of a and the threshold value, a three-month period (March–May 2011 from 12:00 to 12:30 UTC) using lidar data and temperature profiles from the microwave radiometer have been used for PBL height detection using the method based on the WCT and the parcel method respectively. The time interval, around noon, was chosen in order to have high convective activity and a well-mixed PBL. The mean and standard deviation of the PBL height using the parcel method with temperature profiles from the microwave radiometer was 2.2 ± 0.4 km a.s.l. In agreement with results obtained during the comparison of radiosounding and lidar derived PBL heights, the combination $a = 300$ m and 0.05 threshold value provided the best matching between both methods; with PBL height at 2.1 ± 0.7 km a.s.l. and 0.1 ± 0.6 km mean difference during

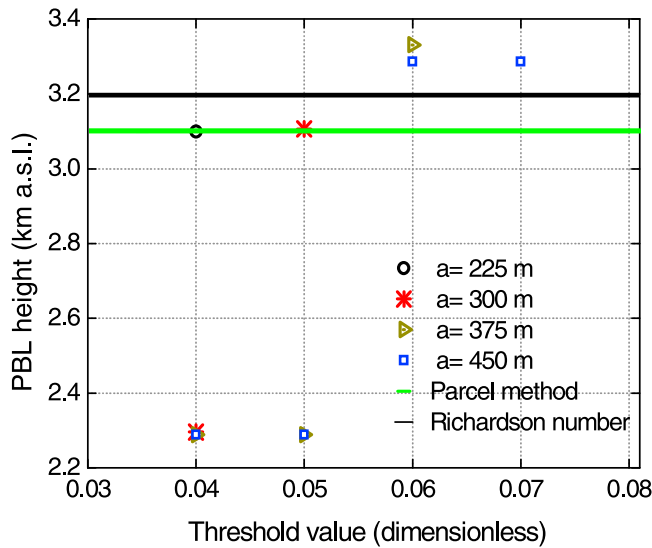


Figure 3. PBL heights obtained from the WCT-based method using different dilations and threshold values, from the parcel method (green line) and the Richardson number method (black line) for 25 July 2011 between 11:00 and 11:30 UTC.

the same period. As obtained from radiosoundings, $a = 225$ m and 0.04 threshold value also provided good results in most cases. From lidar data, the mean PBL height obtained with this combination was 2.0 ± 0.7 km a.s.l. and the mean difference was 0.2 ± 0.7 km. Statistical results of the comparison are shown in Figure 6. Mean values of both combinations are very similar. Nevertheless, the standard deviation is lower for $a = 300$ m. An ANOVA test indicates that mean differences are not significant at the 99% level for any of the combinations. However, the variations are more significant for $a = 225$ m and 0.04 threshold value. The scatterplot of PBL heights from lidar based on the WCT method and from microwave radiometer profiles based on the parcel method indicated a good agreement. The linear fit, intercept forced to zero, show the best agreement (slope = 0.94) for $a = 300$ m

with a 0.98 correlation coefficient. In this way we evidence an average overestimation of the lidar retrieval over the microwave radiometer close to 6%. With $a = 225$ m and 0.04 threshold value the slope was 0.92 and the correlation coefficient 0.97 (figures not shown).

[27] Therefore, from the comparison of the PBL height derived from lidar and microwave radiometer data, optimum parameters for the WCT method were $a = 300$ m and 0.05 threshold value. Although, $a = 225$ m and 0.04 threshold value also provide satisfactory results, previous values were used for automatic PBL detection. Nevertheless, regardless dilation and threshold, the PBL height is sometimes overlooked because the WCT profile does not reach the threshold at any height. It has been checked that the criteria proposed by Brooks [2003] and Morille *et al.*, [2007] were not affected by this problem. However, with the criteria applied in this study, it was also possible to retrieve a feasible PBL height reducing the threshold value by iterating in steps of 0.005, being successful in less than five iterations. In this study, the iteration process was successful for over 50% of the problematic cases.

[28] From the three-month comparison of PBL heights from lidar and microwave radiometer data three scenarios are clearly identified depending on the atmospheric conditions and the presence of lofted aerosol layers above the PBL (Figure 7). The reliability of the method based on the WCT from lidar measurements depends on these scenarios. The first scenario corresponds to atmospheric aerosol from local sources and a well-mixed PBL without stratification. This situation was not very often during spring 2011, only occurring 20% of the dates during the monitoring period. With $a = 300$ m and 0.05 threshold value, PBL heights from lidar were in agreement (difference lower than 250 m) with the ones obtained from the parcel method using the temperature profiles from the microwave radiometer. Figure 7a shows an example of this scenario on 18 March 2011, where the PBL heights from both methods differ less than 100 m. The WCT profile shows a single maximum at 2.3 km a.s.l. clearly identifying the PBL height.

[29] The second scenario corresponds to situations of aerosol from a non-local source clearly decoupled from the PBL with an underlying well-mixed PBL. This situation

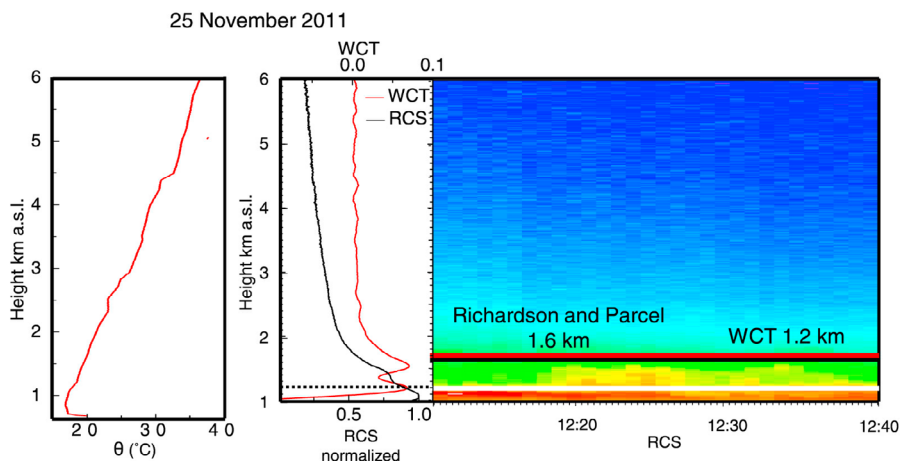


Figure 4. The same as Figure 2a but for 25 November 2011 between 12:10 and 12:40 UTC.

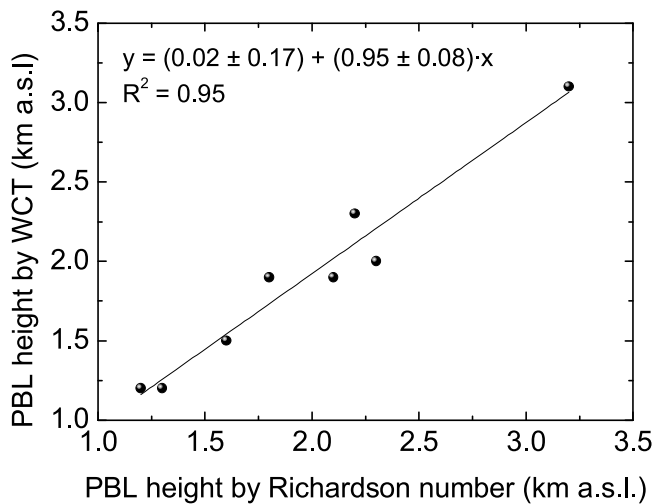


Figure 5. Scatterplot of the PBL heights by the Richardson number method from radiosounding data and by the WCT-based method from lidar data using 300 m dilation and 0.05 threshold value for the eight radiosoundings launched over Granada around midday.

occurred 12% of the dates during the monitoring period. The advection of non-local aerosol, especially African dust intrusions, is quite frequent over the site mainly in spring and summer [Lyamani *et al.*, 2005, 2006]. When the dust layers are clearly decoupled from the PBL this scenario is similar to the previous one, with satisfactory agreement between methods. Differences in PBL height between 25 m and 235 m were found using $a = 300$ m and a 0.05 threshold value. The additional maximum in the WCT profile on 31 March at a higher altitude corresponds to the location of a second aerosol layer over the PBL (Figure 7b).

[30] The third and most complex scenario occurs when the PBL presents stratification (Figure 7c). The WCT method is able to distinguish between the different layers, but it is not feasible to unambiguously identify the PBL height. This situation was quite common during spring 2011, occurring 68% of the dates during the monitoring period. After mixing, when the stratification disappears, the WCT method is able to determine the top of the aerosol layer but it is not always coincident with the top of the PBL if aerosol layers coupled to the PBL exist. This was already reported by other authors and the criteria for the methodology based on the WCT are not always obvious and objective [Wiegner *et al.*, 2006; Pal *et al.*, 2010]. Layers determination was feasible with $a = 300$ m, but in many situations additional information about the daily evolution of the PBL height is needed in order to set the appropriate threshold value. Angelini *et al.* [2009] proposed an algorithm that calculates the PBL height in several intervals during a given period and takes into account differences between the obtained values. A similar procedure applied automatically here could improve the results in the presence of stratification. Moreover, the presence of lofted layers of mineral dust particles also affects the parcel method as the atmospheric temperature profile changes, with lower temperatures near the surface [Santese *et al.*, 2010; Wang *et al.*, 2010] leading to an underestimate of the PBL height. Therefore, since the PBL height is

not always clearly identified, there is a lack of agreement between both methods and the determination of the PBL height becomes less straightforward.

5. One-Year Analysis of the PBL Height Over Granada

[31] The WCT method was used for PBL height detection using lidar measurements at midday from August 2007 to July 2008. From the total number of measurements (220 days) within this period, an automated PBL height detection using the optimized WCT method ($a = 300$ m and 0.05 threshold value) was successful for 178 days. Conversely, the automated procedure failed in 42 days and in 75% of these days the decrease of the signal was not strong enough to fulfill the requirement of having a maximum in the WCT profile for the established threshold value, preventing the detection of PBL height. Under these conditions, a detailed analysis with ancillary data or a readjustment of the threshold value with an iterative procedure as previously described in section 4 is required. The additional 25% failures in the automated PBL height detection occurred in presence of a higher aerosol layer coupled with the PBL, retrieving PBL heights anomalously high. In these latter cases, the WCT method resolves the height of the aerosol layer, but it is not always coincident with the PBL height. The same limitation occurs with derivative methods [Mattis *et al.*, 2004] and additional information is needed for correctly identifying the PBL height.

[32] Figure 8 represents the daily PBL height at midday automatically determined with the WCT method for the 178 successful days as well as mean monthly values at midday from August 2007 to July 2008 over Granada. The mean value for the entire period was 1.7 ± 0.4 km a.s.l., minimum on 17 January 2008 (1.1 km a.s.l.) and maximum on

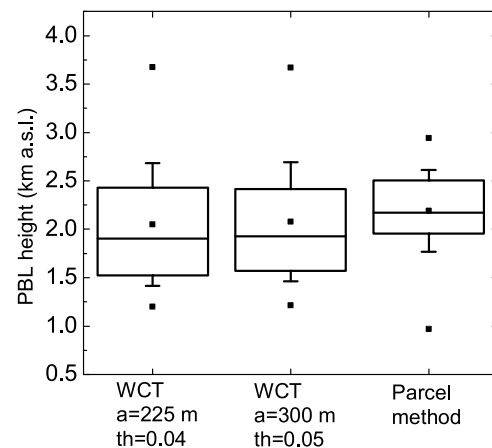


Figure 6. Box plot of the PBL heights during spring 2011 obtained from the WCT-based method for two combinations of the dilation and the threshold value and the parcel method from temperature profiles obtained by the microwave radiometer. In each box central line indicates the median and the extent of boxes, 25 and 75 percentiles; whiskers represent the standard deviation. The central point is the mean value and the external points are the maximum and minimum.

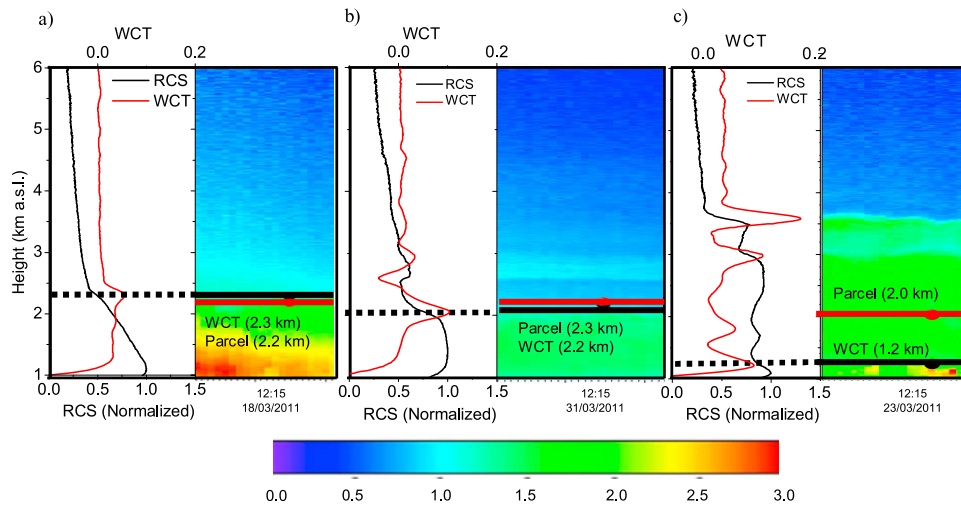


Figure 7. (a) WCT for $a = 300$ m and normalized RCS (arbitrary units) profiles for 18 March 2011 from 12:00 to 12:30 UTC at Granada. The PBL height is indicated by the dotted line. The red and black lines represent the PBL height obtained from the parcel method and the WCT method respectively. (b) The same for 31 March from 12:00 to 12:30 UTC. (c) The same for 23 March 2011 from 12:00 to 12:30 UTC.

23 August (3.1 km a.s.l.). Monthly mean values showed a PBL height higher in June (2.2 km a.s.l.) and lower in January (1.3 km a.s.l.).

[33] The seasonal analysis of the PBL height (Figure 9) revealed higher PBL during summer (June–July–August), with larger variability compare to the other seasons. Values ranged from 1.30 to 3.06 km a.s.l. with a mean value of 2.0 ± 0.6 km a.s.l. Higher PBL heights in summer are mainly related to the occurrence of thermal lows over the Iberian Peninsula that favors a vigorous growth of the PBL [Stull, 1988]. The higher variability of the PBL height during summer was a result of alternating synoptic conditions during this season. Thus the thermal lows favor higher PBL than the high pressure systems. Conversely, winter (December–January–February) showed lower PBL heights from 1.1 to 2.0 km a.s.l. and a mean value of 1.44 ± 0.24 km a.s.l. Variability was lower than in summer. Spring (March–April–May) and autumn (September–October–November) were

very similar, with mean values of 1.7 ± 0.3 and 1.6 ± 0.4 km a.s.l. respectively. More than 90% of the values vary from 1.1 to 2.5 km a.s.l. during both seasons. The seasonal cycle obtained is in agreement with data from central Europe with maximum values in summer and minimum values in winter [Mattis *et al.*, 2004]. Baars *et al.* [2008] obtained mean values of 1.8 km a.s.l. in summer and 0.8 km a.s.l. in winter for a one-year study also over Leipzig (Germany). In Hamburg, about 300 km North and closer to the North Sea, values were 1.8 km a.s.l. for summer and

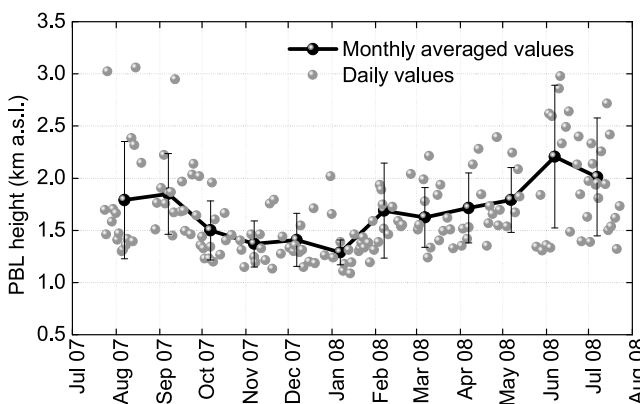


Figure 8. Daily PBL heights and mean monthly values at midday from August 2007 and July 2008 at Granada. Error bars indicate \pm standard deviation.

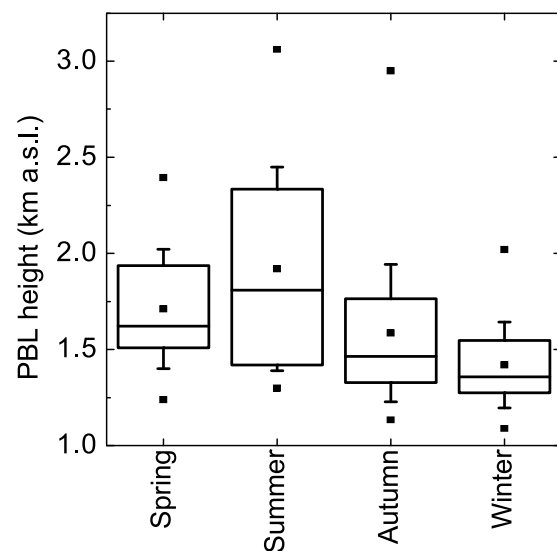


Figure 9. Box plot of seasonal PBL heights at Granada from August 2007 to July 2008. In each box the central line indicates the median and the extent of boxes, 25 and 75 percentiles; whiskers represent the standard deviation. The central point is the mean value and the external points are the maximum and minimum.

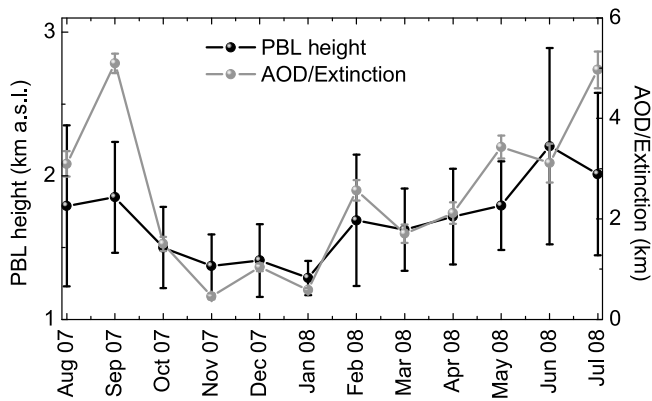


Figure 10. Monthly mean PBL height (black line) and ratio between the aerosol optical depth (AOD) at 675 nm and the surface extinction coefficient at 637 nm at midday from August 2007 to June 2008 at Granada. Error bars indicate \pm standard deviation.

1.1 km a.s.l. for winter [Matthias and Bösenberg, 2002]. It is important to note that Granada is at 680 m a.s.l. while Leipzig and Hamburg are below 100 m a.s.l., therefore the PBL depth is larger in these German cities compared to Granada. Meteorological conditions, especially wind regime and humidity, together with topography may also be related with these differences.

[34] The relationship of the PBL height with the aerosol optical depth and extinction coefficient was also analyzed. Lyamani *et al.* [2010] and Pereira *et al.* [2011] already pointed out the relation between the seasonal cycle of the extinction coefficient and the PBL height. The surface extinction coefficient at 637 nm presented an annual cycle opposite to the PBL height, with a correlation coefficient equal to -0.73 during the study period. In fact, during winter the PBL is lower and therefore the available volume for the vertical dispersion of atmospheric particles is smaller. Moreover, the vertical mixing is less efficient, reinforcing the presence of aerosol near the surface in spite of the lower aerosol load in the atmospheric column (lower aerosol optical depth at 675 nm). In summer, the PBL can reach higher altitudes, allowing additional volume for the dispersion of particles and the vertical mixing of atmospheric aerosol within the PBL. The presence of aerosol near the surface is therefore reduced although the aerosol load in the entire atmospheric column is higher than in winter. It is also possible to check the correlation of PBL height with the ratio between the aerosol optical depth and the extinction coefficient at the surface. This ratio provides an estimate of the aerosol scale height. The scale height parameter arises from the simplified distribution of aerosol particles in the atmosphere used by most radiative transfer models, where an exponential attenuation of atmospheric aerosol concentration with height is assumed [Bokoye *et al.*, 2001]. The aerosol scale height is correlated with the PBL height, with a correlation coefficient of 0.79 during the monitoring period (Figure 10). This confirms the higher presence of particles near the surface when the PBL is shallower even though the

exponential decay is not always strictly fulfilled [Fernández-Gálvez *et al.*, 2012]. This behavior of the aerosol within the PBL is of great importance for the monitoring of air quality.

6. Conclusions

[35] The present study illustrates the capabilities of the WCT method for automated PBL height detection using lidar measurements. The WCT method was optimized by independent measurements using the parcel and the Richardson methods for radiosoundings and the parcel method for simultaneous temperature profiles measured during three months with a ground-based passive microwave radiometer. The analysis of the study period showed three types of scenarios: a clean atmosphere over the PBL with the absence of aerosol layers in the free troposphere, aerosol layers in the free troposphere decoupled from the PBL and stratification due to aerosol layers coupled with the PBL or incomplete mixing. For the first two type of scenarios the automated PBL height detection using the WCT method is successful with optimal results obtained for $a = 300$ m and 0.05 threshold value. There was a good agreement between the three methodologies (parcel, Richardson and WCT-based methods), considering that they are based on different tracers and techniques, with differences below 250 m in the PBL height detection. In the case of multilayering or stratification within the PBL, the methodology based on the WCT is likely to fail for detecting the PBL height, requiring therefore additional information and processing for its determination. Possible methods to be explored in order to solve some of these problems are the use of time frames around the studied interval taking into account the continuity of the PBL height during daytime, as well as an iterative procedure for reducing the threshold value when no maximum is found in the WCT profile.

[36] The automated PBL height detection using lidar measurements from August 2007 to July 2008 over Granada provided satisfactory results for 81% of the days. The annual mean PBL height was 1.7 ± 0.5 km a.s.l., showing higher values in summer (with larger variability) and lower in winter. During spring and autumn mean values are similar with slightly larger variability in autumn.

[37] There was a negative correlation of the PBL height with the aerosol extinction coefficient at 637 nm. The lower PBL height in winter reduces the available volume for vertical dispersion, increasing the extinction coefficient at the surface, in spite of the lower aerosol optical depth. The ratio between the extinction coefficient and the aerosol optical depth at 675 nm is used as an indicator of the scale height, highly correlated with the PBL height.

[38] **Acknowledgments.** This work was supported by the Spanish Ministry of Science and Technology through projects CGL2008-01330-E/CLI (Spanish and Portuguese Aerosol Lidar Network), CGL2010-18782, CSD2007-00067, and FEDER funds under the Complementary Action CGL2011-13580-E/CLI; by the Andalusian Regional Government through projects P10-RNM-6299 and P08-RNM-3568; and by EU through ACTRIS project (EU INFRA-2010-1.1.16-262254). M. J. Granados-Muñoz was funded by the Spanish Ministry of Education under grant AP2009-0552. The authors thank the anonymous reviewers for their comments that have helped to improve the manuscript.

References

- Alados-Arboledas, L., H. Lyamani, and F. J. Olmo (2003), Aerosol size properties at Armilla, Granada (Spain), *Q. J. R. Meteorol. Soc.*, *129*, 1395–1413, doi:10.1256/qj.01.207.
- Angelini, F., F. Barnaba, T. C. Landi, L. Caporaso, and G. P. Gobbi (2009), Study of atmospheric aerosols and mixing layer by LIDAR, *Radiat. Prot. Dosimetry*, *137*, 275–279, doi:10.1093/rpd/ncp219.
- Baars, H., A. Ansmann, R. Engelmann, and D. Althausen (2008), Continuous monitoring of the boundary-layer top with lidar, *Atmos. Chem. Phys.*, *8*, 7281–7296, doi:10.5194/acp-8-7281-2008.
- Bokoye, A. I., A. Royer, N. T. O'Neill, P. Cliche, G. Fedosejevs, P. M. Teillet, and L. J. B. McArthur (2001), Characterization of atmospheric aerosols across Canada from a ground-based sunphotometer network: AEROCAN, *Atmos. Ocean*, *39*, 429–456, doi:10.1080/07055900.2001.9649687.
- Bösenberg, J., et al. (2001), EARLINET: A European aerosol research lidar network, laser remote sensing of the atmosphere, in *Selected Papers of the 20th International Laser Radar Conference*, edited by A. Dabas, C. Loth, and J. Pelon, pp. 155–158, Ed. Ecole Polytech., Palaiseau, France.
- Brooks, I. (2003), Finding boundary layer top: Application of a wavelet covariance transform to lidar backscatter profiles, *J. Atmos. Oceanic Technol.*, *20*, 1092–1105, doi:10.1175/1520-0426(2003)020<1092:FBLTAO>2.0.CO;2.
- Cohn, S. A., and W. M. Angevine (2000), Boundary layer height and entrainment zone thickness measured by lidars and wind-profiling radars, *J. Appl. Meteorol.*, *39*, 1233–1247, doi:10.1175/1520-0450(2000)039<1233:BLHAEZ>2.0.CO;2.
- Eck, T. F., B. N. Holben, J. S. Reid, O. Dubovik, A. Smirnov, N. T. O'Neill, I. Slutsker, and S. Kinne (1999), Wavelength dependence of the optical depth of biomass burning, urban, and desert dust aerosols, *J. Geophys. Res.*, *104*(D24), 31,333–31,349, doi:10.1029/1999JD900923.
- Fernández-Gálvez, J., et al. (2012), Aerosol size distribution from inversion of solar radiances and measured at ground-level during SPAL10 campaign, *Atmos. Res.*, doi:10.1016/j.atmosres.2012.03.015, in press.
- Flamant, C., J. Pelon, P. H. Flamant, and P. Durand (1997), Lidar determination of the entrainment zone thickness at the top of the unstable marine atmospheric boundary-layer, *Boundary Layer Meteorol.*, *83*, 247–284, doi:10.1023/A:1000258318944.
- Guerrero-Rascado, J. L., B. Ruiz Reverter, and L. Alados-Arboledas (2008), Multi-spectral Lidar characterization of the vertical structure of Saharan dust aerosol over Southern Spain, *Atmos. Environ.*, *42*, 2668–2681, doi:10.1016/j.atmosenv.2007.12.062.
- Guerrero-Rascado, J. L., F. J. Olmo, I. Avilés-Rodríguez, F. Navas-Guzmán, D. Pérez-Ramírez, H. Lyamani, and L. Alados-Arboledas (2009), Extreme Saharan dust event over the southern Iberian Peninsula in September 2007: Active and passive remote sensing from surface and satellite, *Atmos. Chem. Phys.*, *9*, 8453–8469, doi:10.5194/acp-9-8453-2009.
- Haefelin, M., et al. (2012), Evaluation of mixing-height retrievals from automated profiling lidars and ceilometers in view of future integrated networks in Europe, *Boundary Layer Meteorol.*, *143*, 49–75, doi:10.1007/s10546-011-9643-z.
- Hayden, K. L., K. G. Anlauf, R. M. Hoff, J. W. Strapp, J. W. Bottenheim, H. A. Wiebe, F. A. Froude, J. B. Martin, D. G. Steyn, and I. G. McKendry (1997), The vertical chemical and meteorological structure of the boundary layer in the Lower Fraser Valley during Pacific '93', *Atmos. Environ.*, *31*, 2089–2105, doi:10.1016/S1352-2310(96)00300-7.
- Holben, B. N., et al. (1998), AERONET—A federated instrument network and data archive for aerosol characterization, *Remote Sens. Environ.*, *66*, 1–16, doi:10.1016/S0034-4257(98)00031-5.
- Holtzlag, B. (2006), GEWEX Atmospheric Boundary Layer Study on stable boundary layers, *Boundary Layer Meteorol.*, *118*, 243–246, doi:10.1007/s10546-005-9008-6.
- Holzworth, C. G. (1964), Estimates of mean maximum mixing depths in the contiguous United States, *Mon. Weather Rev.*, *92*, 235–242, doi:10.1175/1520-0493(1964)092<0235:EOMMMD>2.3.CO;2.
- Hooper, W. P., and E. W. Eloranta (1986), Lidar measurements of wind in the planetary boundary layer: The method, accuracy, and results from joint measurements with radiosonde and kyttoon, *J. Clim. Appl. Meteorol.*, *25*, 990–1001, doi:10.1175/1520-0450(1986)025<0990:LMOWIT>2.0.CO;2.
- Lyamani, H., F. J. Olmo, and L. Alados-Arboledas (2005), Saharan dust outbreak over southeastern Spain as detected by Sun photometer, *Atmos. Environ.*, *39*, 7276–7284.
- Lyamani, H., F. J. Olmo, A. Alcantara, and L. Alados-Arboledas (2006), Atmospheric aerosols during the 2003 heat wave in southeastern Spain I: Spectral optical depth, *Atmos. Environ.*, *40*, 6453–6464, doi:10.1016/j.atmosenv.2006.04.048.
- Lyamani, H., F. J. Olmo, and L. Alados-Arboledas (2008), Light scattering and absorption properties of aerosol particles in the urban environment of Granada, Spain, *Atmos. Environ.*, *42*, 2630–2642, doi:10.1016/j.atmosenv.2007.10.070.
- Lyamani, H., F. J. Olmo, and L. Alados-Arboledas (2010), Physical and optical properties of aerosols over an urban location in Spain: Seasonal and diurnal variability, *Atmos. Chem. Phys.*, *10*, 239–254, doi:10.5194/acp-10-239-2010.
- Mathias, V., and J. Bösenberg (2002), Aerosol climatology for the planetary boundary layer derived from regular lidar measurements, *Atmos. Res.*, *63*, 221–245, doi:10.1016/S0169-8095(02)00043-1.
- Mattis, I., A. Ansmann, D. Müller, U. Wandinger, and D. Althausen (2004), Multiyear aerosol observations with dual-wavelength Raman lidar in the framework of EARLINET, *J. Geophys. Res.*, *109*, D13203, doi:10.1029/2004JD004600.
- Menut, L., C. Flamant, J. Pelon, and P. H. Flamant (1999), Evidence of interaction between synoptic and local scales in the surface layer over the Paris area, *Boundary Layer Meteorol.*, *93*, 269–286, doi:10.1023/A:1002013631786.
- Morille, Y., M. Haefelin, P. Drobinski, and J. Pelon (2007), STRAT: An Automated algorithm to Retrieve the Vertical Structure of the Atmosphere from Single-Channel Lidar Data, *J. Atmos. Oceanic Technol.*, *24*, 761–775, doi:10.1175/JTECH2008.1.
- Murayama, T., et al. (2001), Ground-based network observation of Asian dust events of April 1998 in East Asia, *J. Geophys. Res.*, *106*, 18,345–18,359, doi:10.1029/2000JD900554.
- Navas-Guzmán, F., J. L. Guerrero Rascado, and L. Alados Arboledas (2011), Retrieval of the lidar overlap function using Raman signals, *Opt. Pura Apl.*, *44*(1), 71–75.
- Pal, S., A. Behrendt, and V. Wulfmeyer (2010), Elastic-backscatter-lidar-based characterization of the convective boundary layer and investigation of related statistics, *Ann. Geophys.*, *28*, 825–847, doi:10.5194/angeo-28-825-2010.
- Pereira, S. N., F. Wagner, and A. M. Silva (2011), Seven years of aerosol scattering properties, near the surface, in the southwestern Iberia Peninsula, *Atmos. Chem. Phys.*, *11*, 17–29, doi:10.5194/acp-11-17-2011.
- Rose, T., S. Crewell, U. Löhnert, and C. Simmer (2005), A network suitable microwave radiometer for operational monitoring of the cloudy atmosphere, *Atmos. Res.*, *75*, 183–200, doi:10.1016/j.atmosres.2004.12.005.
- Santese, M., M. R. Perrone, A. S. Zakey, F. De Tomasi, and F. Giorgi (2010), Modeling of Saharan dust outbreaks over the Mediterranean by RegCM3: Case studies, *Atmos. Chem. Phys.*, *10*, 133–156, doi:10.5194/acp-10-133-2010.
- Seibert, P., F. Beyrich, S.-E. Gryning, S. Joffre, A. Rasmussen, and P. Tercier (2000), Review and intercomparison of operational methods for the determination of the mixing height, *Atmos. Environ.*, *34*(7), 1001–1027, doi:10.1016/S1352-2310(99)00349-0.
- Sicard, M., C. Pérez, F. Rocadenbosch, J. M. Baldasano, and D. García-Vizcaino (2006), Mixed-layer depth determination in the Barcelona coastal area from regular Lidar measurements: Methods, results and limitations, *Boundary Layer Meteorol.*, *119*, 135–157, doi:10.1007/s10546-005-9005-9.
- Steyn, D., M. Baldi, and R. M. Hoff (1999), The detection of mixed layer depth and entrainment zone thickness from lidar backscatter profiles, *J. Atmos. Oceanic Technol.*, *16*, 953–959, doi:10.1175/1520-0426(1999)016<0953:TDOMLD>2.0.CO;2.
- Stull, R. B. (1988), *An Introduction to Boundary Layer Meteorology*, Kluwer Acad., Dordrecht, Netherlands.
- Vaughan, M., D. Winker, and K. Powell (2005), CALIOP Algorithm Theoretical Basis Document, part 2, Feature Detection and Layer Properties Algorithms, *Rep. PC-SCI-202.01*, NASA Langley Res. Cent., Hampton, Va. [Available at http://www-calipso.larc.nasa.gov/resources/project_documentation.php.]
- Vogelezang, D. H. P., and A. A. M. Holtzlag (1996), Evolution and model impacts of alternative boundary layer formulations, *Boundary Layer Meteorol.*, *81*, 245–269, doi:10.1007/BF02430331.
- Wang, H., X. Zhang, S. Gong, Y. Chen, G. Shi, and W. Li (2010), Radiative feedback of dust aerosols on the East Asian dust storms, *J. Geophys. Res.*, *115*, D23214, doi:10.1029/2009JD013430.
- Welton, E. J., J. R. Campbell, J. D. Spinhirne, and V. S. Scott (2001), Global monitoring of clouds and aerosols using a network of micro-pulse lidar systems, in *Lidar Remote Sensing for Industry and Environmental Monitoring*, edited by U. N. Singh, T. Itabe, and N. Sugimoto, pp. 151–158, SPIE, Bellingham, Wash.
- Wiegner, M., S. Emeis, V. Freudenthaler, B. Heese, W. Junkermann, C. Munkel, K. Schafer, M. Seefeldner, and S. Vogt (2006), Mixing layer height over Munich, Germany: Variability and comparisons of different methodologies, *J. Geophys. Res.*, *111*, D13201, doi:10.1029/2005JD006593.